

Exclusive meson production at COMPASS

Paweł Sznajder (on behalf of the COMPASS Collaboration)*†

National Centre for Nuclear Research, Warsaw

E-mail: pawel.sznajder@ncbj.gov.pl

The recent measurements of exclusive vector meson production performed by the COMPASS Collaboration are presented. In particular, recent results on single-spin and double-spin asymmetries for exclusive ρ^0 and ω production measured on a transversely polarised proton target are shown. Some of these asymmetries are sensitive to the GPDs E , which are related to the orbital angular momenta of quarks. Other asymmetries are sensitive to the chiral-odd GPDs H_T , which are related to the transversity PDF distributions. The results for ρ^0 mesons provide the first experimental evidence from hard exclusive vector meson production for the existence of non-vanishing GPDs H_T . The results for ω mesons are sensitive to the pion pole contribution to the production mechanism. The future measurements of hard exclusive meson production at COMPASS are also discussed.

*XXIII International Workshop on Deep-Inelastic Scattering
27 April - May 1 2015
Dallas, Texas*

*Speaker.

†Speaker supported by the Polish NCN Grant DEC-2011/01/M/ST2/02350.

1. Introduction

Hard exclusive electro- and muoproduction of mesons on nucleons has played an important role in studies of the hadron structure and recently gained renewed interest as it allows access to generalised parton distributions (GPDs). The GPDs provide a novel and comprehensive description of the partonic structure of the nucleon and contain a wealth of new information. For instance the GPDs give a description of the nucleon as an extended object, referred to as 3-dimensional nucleon tomography, and give an access to the orbital angular momentum of quarks.

At leading twist the chiral-even GPDs H and E are sufficient to describe exclusive vector meson production on a spin-1/2 target. These GPDs are of special interest as they are related to the total angular momentum carried by partons in the nucleon [1]. The GPDs H are well constrained in the accessible x_{Bj} range by HERA, HERMES and JLAB data. The constraints on the GPDs E are weak and come mainly from measurements of the nucleon Pauli form factor. There exist also the chiral-odd, "transverse" GPDs, in particular H_T and \bar{E}_T . It was shown in Refs. [2, 3] that they are required to describe exclusive scalar meson production on transversely polarised protons.

In following we summarise recent measurements of the transverse target spin asymmetries for exclusive ρ^0 and ω meson production. The comparison between these mesons is of special interest as they probe different combinations of the GPDs for u and d quarks. The measured observables are sensitive both to the chiral-even and chiral-odd GPDs. At the COMPASS kinematics exclusive ω production is also sensitive to the pion pole contribution to the production mechanism [4]. The interpretation of results for both mesons is done in the framework of the GPD-based model proposed by Goloskokov and Kroll [4, 5]. Planned measurements of exclusive meson production, which are a part of the approved COMPASS-II proposal [6], are also discussed.

2. Formalism

For exclusive meson production off a transversely polarised target five single (UT) and three double (LT) spin asymmetries can be defined. These are

$$\begin{aligned}
 A_{\text{UT}}^{\sin(\phi-\phi_s)} &= -\frac{\text{Im}(\sigma_{++}^{+-} + \varepsilon\sigma_{00}^{+-})}{\sigma_0}, & A_{\text{LT}}^{\cos(\phi-\phi_s)} &= \frac{\text{Re}\sigma_{++}^{+-}}{\sigma_0}, & A_{\text{UT}}^{\sin(\phi+\phi_s)} &= -\frac{\text{Im}\sigma_{+-}^{+-}}{\sigma_0}, \\
 A_{\text{UT}}^{\sin(2\phi-\phi_s)} &= -\frac{\text{Im}\sigma_{+0}^{-+}}{\sigma_0}, & A_{\text{LT}}^{\cos(2\phi-\phi_s)} &= -\frac{\text{Re}\sigma_{+0}^{-+}}{\sigma_0}, & A_{\text{UT}}^{\sin(3\phi-\phi_s)} &= -\frac{\text{Im}\sigma_{+-}^{-+}}{\sigma_0}, \\
 A_{\text{UT}}^{\sin\phi_s} &= -\frac{\text{Im}\sigma_{+0}^{+-}}{\sigma_0}, & A_{\text{LT}}^{\cos\phi_s} &= -\frac{\text{Re}\sigma_{+0}^{+-}}{\sigma_0}.
 \end{aligned} \tag{2.1}$$

The photoabsorption cross sections or the interference terms, σ_{mn}^{ij} , are proportional to the bilinear combinations of the helicity amplitudes, \mathcal{M} , for the photoproduction subprocess $\gamma^* p \rightarrow \rho^0 p$,

$$\sigma_{mn}^{ij} \propto \sum \mathcal{M}_{m'i',mi}^* \mathcal{M}_{m'i',nj}, \tag{2.2}$$

where the helicity of the virtual photon is denoted by $m, n = -1, 0, +1$ and the helicity of the initial-state proton is given by $i, j = -1/2, +1/2$ (in Eq. (2.1) and in the following these helicities are labelled by only their signs or zero). The sum runs over all spin combinations for the final state,

given by the spin of the meson, $m' = -1, 0, +1$, and the spin of the final-state proton, $i' = -1/2, +1/2$. For brevity a dependence on the kinematic variables is omitted here.

The total unpolarised cross section, σ_0 , is given by the sum of cross sections for longitudinally, σ_L , and transversely, σ_T , polarised virtual photons,

$$\sigma_0 = \frac{1}{2} (\sigma_{++}^{++} + \sigma_{++}^{--}) + \varepsilon \sigma_{00}^{++} = \sigma_L + \varepsilon \sigma_T, \quad (2.3)$$

where the virtual photon polarisation parameter can be approximated by $\varepsilon \simeq (1-y)/(1-y+y^2/2)$.

Each asymmetry is related to a specific modulation of the cross section in ϕ and ϕ_s angles indicated by the superscript. The angle ϕ is the azimuthal angle between the lepton plane, given by the incoming and scattered lepton momenta, and the hadron plane, given by the virtual photon and meson momenta. The angle ϕ_s is the azimuthal angle around the virtual photon momentum between the lepton plane and the spin direction of the target nucleon. The complete formula for the cross section can be found in Ref. [7]. The asymmetries are extracted from the data selected as described in the following.

3. COMPASS experiment

The COMPASS experiment (Common Muon Proton Apparatus for Structure and Spectroscopy) is situated at the high-intensity M2 muon beam line of the CERN SPS. A detailed description of the apparatus can be found in Ref. [8].

During the taking of data used in the analyses referred in this paper, the μ^+ beam had the nominal momentum of 160 GeV/c with the spread of 5% and the longitudinal polarisation of 80%. The data were taken at the mean intensity of $3.5 \cdot 10^8 \mu^+$ /spill, for the spill length of about 10 s every 40 s. A measurement of the trajectory and the momentum was performed upstream the target for each incoming muon.

The muon beam was scattered off an ammonia target (NH₃) containing transversely polarised protons. The polarisation was obtained by the Dynamic Nuclear Polarisation method and was about 90%. The dilution factor, which is the cross-section-weighted fraction of the polarisable material, was about 25%. To minimise systematic effects due to a possible spectrometer instability and an acceptance variation, the target was divided into three cells, where the target material inside the consecutive cells had the opposite polarisation. The polarisation of the whole target was being reversed periodically.

The COMPASS spectrometer is a 50 m long two stage spectrometer with excellent capability for tracking and particle identification. Each stage of the spectrometer has a dipole magnet with tracking detectors before and after the magnet. In total, the spectrometer is equipped with about 300 tracking detector planes, which provide a high redundancy for the reconstruction. There are also several particle identification systems. An identification of hadrons is provided by a large Ring Imaging Cherenkov detector (RICH) installed in the first stage of the spectrometer. Both stages are equipped with the so-called muon walls for an identification of muons. Each wall consists of a hadron absorber placed between two hodoscope stations. A coincidence in those hodoscopes is used for the muon identification. In addition, each stage is equipped with a pair of electromagnetic and hadron calorimeters. The electromagnetic calorimeters are crucial for the analysis of exclusive

ω production, as they allow for the reconstruction of π^0 mesons coming from the $\omega \rightarrow \pi^+\pi^-\pi^0$ decay.

4. Event selection

To determine the transverse target spin asymmetries for exclusive production of ρ^0 meson the data taken in 2007 and 2010 with polarised protons were analysed. Each selected event contains a primary vertex with only one incoming and one outgoing muon track and with only two outgoing hadron tracks of opposite charges. It is assumed that the outgoing hadrons are pions. The ρ^0 resonance is selected by the cut on the reconstructed invariant mass, $0.5 \text{ GeV}/c^2 < M_{\pi^+\pi^-} < 1.1 \text{ GeV}/c^2$.

The analysis of exclusive ω production was performed for the data taken in 2010 with the transversely polarised proton target. Each selected event contains a primary vertex with the same topology as described for the aforementioned ρ^0 reconstruction. In addition, only two clusters must be reconstructed in the electromagnetic calorimeters, which are timely correlated to the vertex and that are not associated to any charged particle. These clusters are assumed to be caused by a pair of photons emitted from the primary vertex. The cut on the invariant mass of two photons, $M_{\gamma\gamma}$, depends on the sum of photon energies. It is because the ECAL resolution, and therefore the width of π^0 peak, depends on the energy of a single photon. The ω resonance is selected by the cut on the reconstructed invariant mass, $|M_{\pi^+\pi^-\pi^0} - M_{\omega}^{\text{PDG}}| < 0.07 \text{ GeV}/c^2$, where $M_{\omega}^{\text{PDG}} \approx 0.783 \text{ GeV}/c^2$.

Because recoiling target particle is undetected, the exclusivity is checked by the missing energy, $E_{\text{miss}} = ((p + q - v)^2 - p^2)/2M_p$, where M_p is the proton mass and p , q and v are the four-momenta of proton, photon and meson, respectively. For exclusive events the reconstructed values of E_{miss} are close to zero. To select these events the cuts $|E_{\text{miss}}| < 2.5 \text{ GeV}$ and $|E_{\text{miss}}| < 3.0 \text{ GeV}$ are used, for the ρ^0 and ω measurements, respectively. The cut $0.05 \text{ (GeV}/c)^2 < p_T^2 < 0.5 \text{ (GeV}/c)^2$ is applied in both measurements, where p_T^2 is the meson squared transverse momentum with respect to the virtual photon direction. The lower cut on p_T^2 suppresses a contribution from the coherent production on the target nuclei, while the upper cut provides a further reduction of the non-exclusive background.

The kinematic region is defined by the following cuts: $1 \text{ (GeV}/c)^2 < Q^2 < 10 \text{ (GeV}/c)^2$, $0.1 < y < 0.9$, $0.003 < x_{Bj} < 0.35$, $W > 5 \text{ GeV}/c^2$ (invariant mass of the virtual photon - nucleon system) and p_T^2 cuts as indicated above. In the analysis of ρ^0 meson the asymmetries were extracted by using the 2D binned likelihood method after a subtraction of the remaining semi-inclusive background. In the analysis of ω meson the signal and background asymmetries were extracted simultaneously with the unbinned likelihood method.

5. Results and discussion

The mean values of asymmetries measured for exclusive ρ^0 meson production are shown in Fig. 1. They are given for the mean values of kinematic variables, $\langle Q^2 \rangle = 2.2 \text{ (GeV}/c)^2$, $\langle x_{Bj} \rangle = 0.039$, $\langle p_T^2 \rangle = 0.2 \text{ (GeV}/c)^2$, $\langle W \rangle = 8.1 \text{ GeV}/c^2$ and $\langle y \rangle = 0.24$, of the selected data set. The asymmetry $A_{UT}^{\sin\phi_s}$ was found to be $-0.019 \pm 0.008 \text{ (stat)} \pm 0.003 \text{ (sys)}$ and all other asymmetries were found to be small, consistent with zero within experimental uncertainty. The

asymmetries measured as a function of Q^2 , x_{Bj} or p_T^2 can be found in Ref. [9], together with a comparison to predictions of the GPD-based model proposed by Goloskokov and Kroll [8, 10]. The model agrees well with our data.

For an interpretation of the shown results of particular interest are the following asymmetries, for which the dependence on the helicity amplitudes reads

$$\begin{aligned}\sigma_0 A_{UT}^{\sin(\phi-\phi_s)} &= -2\text{Im} \left[\varepsilon \mathcal{M}_{0-,0+}^* \mathcal{M}_{0+,0+} + \mathcal{M}_{+-,++}^* \mathcal{M}_{+,++} + \frac{1}{2} \mathcal{M}_{0-,++}^* \mathcal{M}_{0+,++} \right], \\ \sigma_0 A_{UT}^{\sin(2\phi-\phi_s)} &= -\text{Im} \left[\mathcal{M}_{0+,++}^* \mathcal{M}_{0-,0+} \right], \\ \sigma_0 A_{UT}^{\sin\phi_s} &= -\text{Im} \left[\mathcal{M}_{0-,++}^* \mathcal{M}_{0+,0+} - \mathcal{M}_{0+,++}^* \mathcal{M}_{0-,0+} \right].\end{aligned}\quad (5.1)$$

The dominant contribution from the $\gamma_L^* \rightarrow \rho_L^0$ transition is given by $\mathcal{M}_{0+,0+}$ and $\mathcal{M}_{0-,0+}$ helicity amplitudes, which are related to the chiral-even GPDs H and E , respectively. The suppressed contribution from the $\gamma_T^* \rightarrow \rho_T^0$ transition is given by $\mathcal{M}_{+,++}$ and $\mathcal{M}_{+-,++}$ helicity amplitudes, which are also related to the chiral-even GPDs. Description of the $\gamma_T^* \rightarrow \rho_L^0$ transition is possible by an inclusion of the chiral-odd GPDs H_T and \bar{E}_T , which are related to $\mathcal{M}_{0-,++}$ and $\mathcal{M}_{0+,++}$ helicity amplitudes, respectively. The $\gamma_L^* \rightarrow \rho_T^0$ and $\gamma_T^* \rightarrow \rho_{-T}^0$ transitions are known to be suppressed and are neglected in this formalism.

The vanishing $A_{UT}^{\sin(\phi-\phi_s)}$ asymmetry is interpreted as a cancellation of the GPDs E^u and E^d due to their different sign but similar magnitude. A contribution of the chiral-odd GPDs is negligible here, as one can see from comparison of calculations of Refs. [5] and [11]. The $A_{UT}^{\sin\phi_s}$ asymmetry represents an imaginary part of two bilinear products of helicity amplitudes. The first product is related to the GPDs H and H_T , while the second one is related to the GPDs E and \bar{E}_T . The latter product appears also in the $A_{UT}^{\sin(2\phi-\phi_s)}$ asymmetry. The $A_{UT}^{\sin\phi_s}$ asymmetry is found to be different from zero, while the $A_{UT}^{\sin(2\phi-\phi_s)}$ asymmetry vanishes. It implies non-negligible contribution of the GPDs H_T . It is the first experimental evidence from hard exclusive ρ^0 production for the observation of these chiral-odd GPDs.

All eight transverse target asymmetries for exclusive ω meson production are shown in Fig. 2 (left). They are given for the mean values of kinematic variables, $\langle Q^2 \rangle = 2.2$ (GeV/c)², $\langle x_{Bj} \rangle = 0.049$, $\langle p_T^2 \rangle = 0.17$ (GeV/c)², $\langle W \rangle = 7.1$ GeV/c² and $\langle y \rangle = 0.18$, of the selected data set. The single spin asymmetries measured as a function of Q^2 , x_{Bj} or p_T^2 are shown in Fig. 2 (right).

In Fig. 2 (right) the measured asymmetries are compared to the predictions of the Goloskokov-Kroll model [4, 10]. The authors have provided three sets of predictions: one without the pion pole contribution and two with the contribution that differ by the sign of $\pi\omega$ form factor. While the

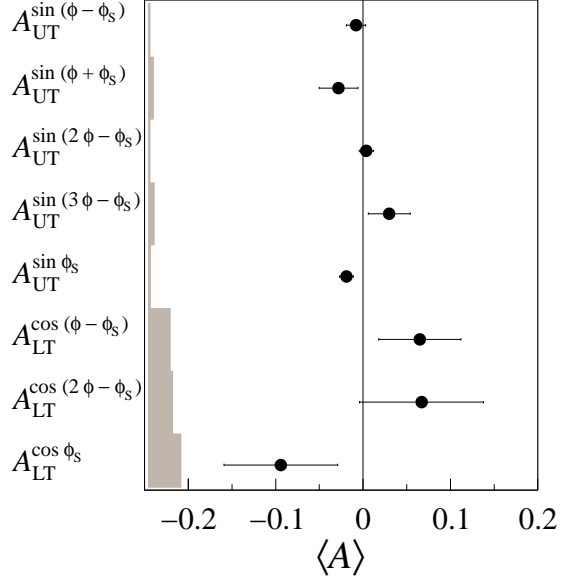


Figure 1: The azimuthal asymmetries for exclusive ρ^0 meson production on transversely polarised protons. The error bars (left bands) represent the statistical (systematic) uncertainties. Mean values of kinematic variables are indicated in the text.

results for $A_{UT}^{\sin(\phi-\phi_s)}$ and $A_{UT}^{\sin(\phi+\phi_s)}$ asymmetries prefer the positive sign of $\pi\omega$ form factor, the results for $A_{UT}^{\sin\phi_s}$ asymmetry prefer the negative sign. At present the reason for this discrepancy between the model and the experimental data is unknown. The remaining asymmetries are not sensitive to the sign of $\pi\omega$ form factor.

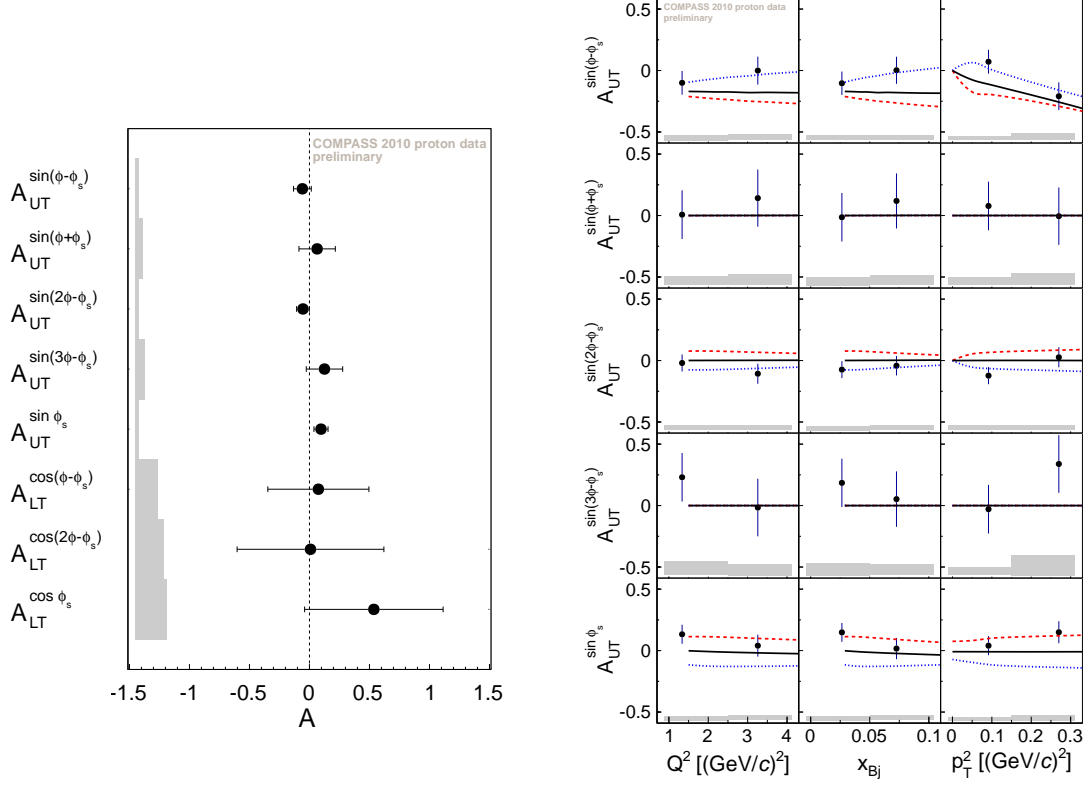


Figure 2: Left: The azimuthal asymmetries for exclusive ω meson production on transversely polarised protons. The error bars (left bands) represent the statistical (systematic) uncertainties. Mean values of kinematic variables are indicated in the text. Right: Single spin azimuthal asymmetries for exclusive ω meson production on transversely polarised protons. The curves show the predictions of the GPD-based model [4, 10]. The dashed red and dotted blue curves represent the predictions with the positive and negative $\pi\omega$ form factors, respectively, while the solid black curve represents the predictions without the pion pole.

6. Future measurements at COMPASS-II

The GPD program at COMPASS is continued. The COMPASS-II proposal [6] of the new measurements has been already approved by CERN. Measurement of exclusive meson production on unpolarised target is one of the main goals of this proposal, together with the measurement of DVCS. The data for the GPD program at COMPASS-II were successfully taken during 2012 pilot run and will be taken in 2016-2017.

For purpose of the GPD program at COMPASS-II the apparatus has been optimised for measurements of exclusive reactions. In particular, new equipment has been build, like a new large angle electromagnetic calorimeter to cover high x_{Bj} region for the DVCS measurement (ECAL0,

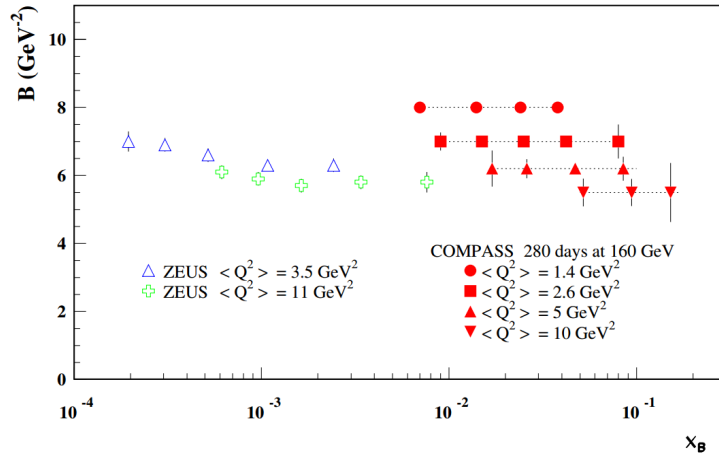


Figure 3: The projection of b slope measurement for exclusive ρ^0 production for the planned 2016-2017 data taking. Also existing data points from ZEUS in a similar Q^2 range are shown.

$1/3$ ready in 2012) and a 2.5 m long liquid hydrogen target surrounded by a 4 m long recoil proton detector (CAMERA).

For the COMPASS-II proposal projections of expected results were made. One of the projections was made in order to evaluate expected precision for the measurement of b slope of $d\sigma/dt$ cross section as a function of x_{Bj} for exclusive ρ^0 meson production. Here, t is one of Mandelstam variables. The slope is related to the transverse size of the nucleon and thus it can be used for the nucleon tomography. The projection of measurement of slope in four bins of Q^2 for 2016-2017, together with existing data points from ZEUS in a similar Q^2 range, is shown in Fig. 3.

References

- [1] X. Ji, Phys. Rev. Lett. **78** (1997) 610
- [2] S.V. Goloskokov and P. Kroll, Eur. Phys. J. **C65** (2010) 137
- [3] S.V. Goloskokov and P. Kroll, Eur. Phys. J. **A47** (2011) 112
- [4] S.V. Goloskokov and P. Kroll, Eur. Phys. J. **A50** (2014) 146
- [5] S.V. Goloskokov and P. Kroll, Eur. Phys. J. **C74** (2014) 2725
- [6] The COMPASS Collaboration, CERN-SPSC-2010-014
- [7] M. Diehl and S. Sapeta, Eur. Phys. J. **C41** (2005) 515
- [8] The COMPASS Collaboration, Nucl. Instrum. Meth. **A577** (2007) 455
- [9] The COMPASS Collaboration, Phys. Lett. **B731** (2014) 19
- [10] S.V. Goloskokov and P. Kroll, private communication
- [11] S.V. Goloskokov and P. Kroll, Eur. Phys. J. **C59** (2009) 809